

See discussions, stats, and author profiles for this publication at: <https://www.researchgate.net/publication/263961309>

Computational Modeling of Stark Effects in Organic Dye-Sensitized TiO₂ Heterointerfaces

ARTICLE *in* JOURNAL OF PHYSICAL CHEMISTRY LETTERS · MAY 2011

Impact Factor: 7.46 · DOI: 10.1021/jz200443w

CITATIONS

36

READS

21

2 AUTHORS:



Mariachiara Pastore

Italian National Research Council

52 PUBLICATIONS 1,248 CITATIONS

SEE PROFILE



Filippo De Angelis

Università degli Studi di Perugia

265 PUBLICATIONS 11,207 CITATIONS

SEE PROFILE

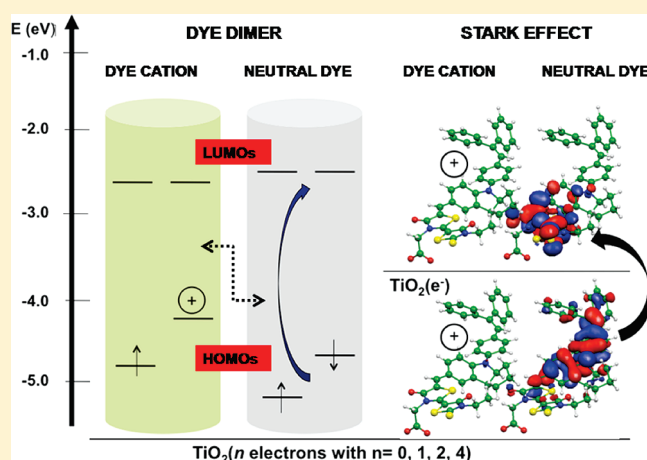
Computational Modeling of Stark Effects in Organic Dye-Sensitized TiO₂ Heterointerfaces

Mariachiara Pastore and Filippo De Angelis*

Istituto CNR di Scienze e Tecnologie Molecolari c/o Dipartimento di Chimica, Università di Perugia, via Elce di Sotto 8, I-06123 Perugia, Italy

ABSTRACT: We report a computational modeling study, based on DFT and time-dependent DFT techniques, to investigate the origin and the effect of local electric fields on the optical properties of organic dye-sensitized heterointerfaces, examining the case of the indoline D149 sensitizer on TiO₂. On the one hand, we give precise information about the anchoring mode of D149 and its orientation with respect to the TiO₂ surface, and on the other hand, we provide the computational framework model to interpret the Stark shifts experimentally observed by PIA spectroscopy. Our results show that the presence of oxidized dye molecules induces major spectral changes on the adjacent neutral dyes, which, along with the simulated effect of injected charge into TiO₂, provide Stark shifts nicely reproducing the experimental observations.

SECTION: Energy Conversion and Storage



In the last two decades, dye-sensitized solar cells (DSCs), introduced by O'Regan and Grätzel in 1991,^{1–4} have attracted an increasing interest as potential low-cost alternatives to the traditional silicon-based photovoltaic systems. In these devices, dye molecules, attached to a wide band gap semiconductor electrode consisting of a mesoporous oxide layer, are responsible for sunlight absorption. Upon dye excitation, four events sequentially occur, (i) the instantaneous intermolecular charge transfer (CT) from the dye donor to its acceptor moiety, (ii) the ultrafast (fs to ps time scale) electron injection from the dye excited state into the TiO₂ manifold of unoccupied states, (iii) the regeneration of the oxidized dye by the reduced electrolyte species (usually I[–]), taking place in the μ s time domain, and (iv) regeneration of the oxidized electrolyte (I₃[–]) at the cathode to close the circuit.

Although the most efficient DSC devices based on the liquid I[–]/I₃[–] electrolyte are still those employing Ru(II)-based dyes, such as N3 and N719,^{3,5} a number of promising push–pull metal-free dyes, allowing simpler and lower-cost preparation processes as well as larger structural variety, have been developed,^{6–9} with overall efficiencies approaching 10%.^{10–12} Moreover, in conjunction with ferrocene or cobalt-based electrolytes, organic dyes have been shown to clearly outperform Ru(II)-based dyes.^{13–16}

Organic sensitizers are most commonly based on a dipolar D– π –A architecture; the donor group (D), usually lying away from the oxide surface, is an electron-rich unit, linked through a π bridge spacer to the electron-acceptor group (A), which is directly bound to the TiO₂ surface, usually through a carboxylic or cyanoacrylic function. This peculiar push–pull structure

guarantees a good electronic coupling between the dye excited state and the TiO₂ manifold of unoccupied states, which is essential for efficient electron injection, as well as to slow down back parasitic recombination reactions occurring between injected electrons and dye cations and/or oxidized species in the electrolyte.

The kinetics of the processes occurring in the DSC can be conveniently investigated by means of transient absorption spectroscopy,^{17–19} where the sample is excited by a pulsed laser or by photoinduced absorption (PIA) spectroscopy,^{20,21} where, instead, the differential absorption with and without excitation of a sample is measured.

Recently, transient spectroscopy studies^{22–28} on working devices have been focused on the effects that local electric fields seem to induce on the ground-state absorption spectrum of the semiconductor-adsorbed dyes. These effects manifest themselves as absorbance changes occurring for the neutral, nonoxidized, adsorbed dyes, which have been detected by both transient absorption and PIA spectroscopy. Various interpretations have been adduced to explain the observed band shifts and intensity changes. Staniszewski et al.²⁵ attributed the spectral changes to a marked change occurring in the dye environment after electron injection and regeneration by iodide, essentially due to slow cations transfer; basically, electron injection perturbs the electrostatic environment surrounding the dye, which slowly responds by displacing positive charges due to solution or surface-adsorbed

Received: April 2, 2011

Accepted: May 3, 2011

Published: May 10, 2011

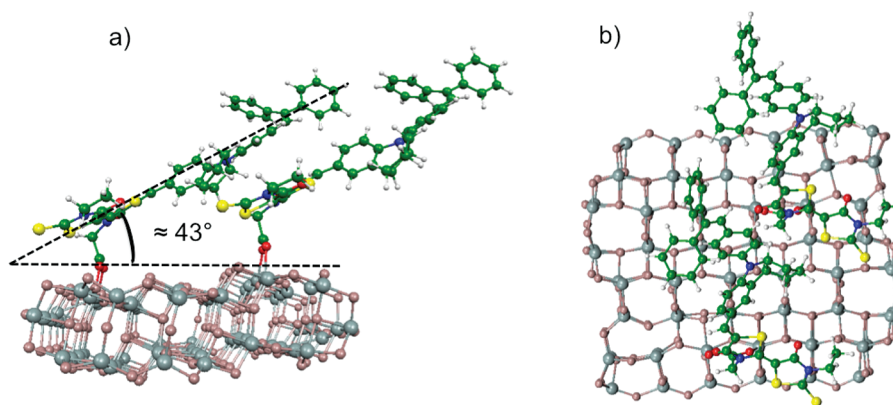


Figure 1. Side view (a) and top view (b) of the optimized adsorption geometry and relative inclination of D149 on the (101) $(\text{TiO}_2)_{82}$ anatase cluster.

Li^+ ions or protons. The appearance of similar or related peak bleaches in the adsorbed dye absorption spectrum has also been ascribed to possible phenomena of electron accumulation into the semiconductor affecting the LUMO of the dye²⁷ or electron extraction²⁸ from the TiO_2 as well as to the presence of long-lived photoreduced dye molecules.²⁶ However, more recently, some authors argued^{22–24} that the measured spectral changes are consistent with first-order transient Stark effects,^{29–31} already shown to take place in semiconductor nanocrystallites^{32,33} and metal complexes^{34–36} but thought to be negligible in DSCs due to the high ionic strength of the electrolyte solution or of the highly doped hole conductor and to the large electrical permittivity of TiO_2 . Such local electric fields, which show maximum amplitude at the initial observation times after electron injection, are expected to be associated with the electron transfer from the dye to the TiO_2 film and to the consequential formation of oxidized dye molecules.

In first-order Stark effects, the change in transition frequency is proportional to the change in dipole moment between the ground and excited states of the molecule ($\Delta\nu \propto -\Delta\mu$),³¹ and it can be shown (see ref 24 for the detailed derivation) that when the external field is perpendicular to the substrate, the change in absorbance (ΔA) is proportional to the change in the dipole component normal to the TiO_2 surface (hereafter termed $\Delta\mu_z$). By using PIA, Cappel et al.²⁴ have designed an elegant experimental setup based on the application of an electric field normal to the surface of a flat TiO_2 electrode and examined the case of two organic dyes. These authors considered the indoline dye D149^{7,10} and the P1 dye,³⁷ which are respectively employed in n-type and p-type DSC devices. The two dyes are indeed characterized by CT excited states pointing in opposite directions with respect to the semiconductor surface and are thus expected to show opposite Stark band shifts. For an ordered monolayer of dyes anchored to a flat TiO_2 surface, the measured changes in absorbance due to the Stark effect and the related estimate of $\Delta\mu_z$ can also be exploited to obtain an indication of the relative orientation of the dye molecule with respect to the oxide surface.²⁴

In general, determining the dye anchoring mode on the semiconductor surface is of crucial importance for understanding the detailed factors affecting DSC efficiency as the bonding type and the extent of electronic coupling between the dye's excited state and the semiconductor conduction band (CB), as well as the dye dipole moment, directly influence the cell performances.³⁸ From an experimental standpoint, the dye adsorption

mode is usually investigated by Fourier transform infrared (FT-IR) spectroscopy and surface-enhance Raman spectroscopy (SERS),^{39–47} whereby the characteristic signals of the symmetric and asymmetric stretching of the dye carboxylic anchoring groups are used as a diagnostic of their interaction with the semiconductor surface.⁴⁸ More recently, photoelectron spectroscopy (PES) has also been employed to characterize the dye/ TiO_2 interface,^{49–51} providing information about the orientation (flat or perpendicular) of adsorbed dyes molecules with respect to the TiO_2 surface.

Motivated by the very recent work of Cappel et al.²⁴ and by our previous work on the adsorption and aggregation of the D149 dye on TiO_2 surfaces,⁵² in this Letter, we report a computational modeling investigation, based on density functional theory (DFT) and time-dependent DFT (TD-DFT) techniques, to investigate the effect of local electric fields on the optical properties of organic dye-sensitized heterointerfaces. On the one hand, we provide precise information about the anchoring mode of D149 and its orientation with respect to the TiO_2 surface, and on the other hand, we provide the computational framework model to interpret the experimental Stark shifts reported in ref 24. Our approach consists of “statically” simulating the oxidation/electron injection and regeneration steps and the associated optical responses in a prototypical model consisting of the most stable dimeric configuration of D149 adsorbed on a TiO_2 slab.⁵²

Owing to our realistic models and high-level computational approach, we are able to quantitatively reproduce the measured Stark shifts for D149 and provide a clear picture of the role that different contributions play in inducing such spectral changes.

First, we briefly discuss the adsorption geometry of D149 and of its preferred dimeric configuration, (2,2)-D149, on the $(\text{TiO}_2)_{82}$ cluster, reported in Figure 1. In ref 52, after examining both monodentate and bidentate binding modes for the stand-alone dye, we concluded that a bidentate anchoring mechanism with proton transfer to a nearby surface oxygen is occurring, this structure being energetically favored compared to the monodentate one. These results are in line with the conclusions by Howie et al.⁵³ and those reported by Cappel et al.²⁴ on the basis of the small $\Delta\mu_z$ of ~ 1 D obtained from the PIA measurements.

In fact, we recall that the change between the ground and excited states in the component of the dipole moment normal to the TiO_2 surface, $\Delta\mu_z$, can be used to discriminate between the monodentate (molecule standing up) and the bidentate (molecule laying flat) coordination modes. In the former case,

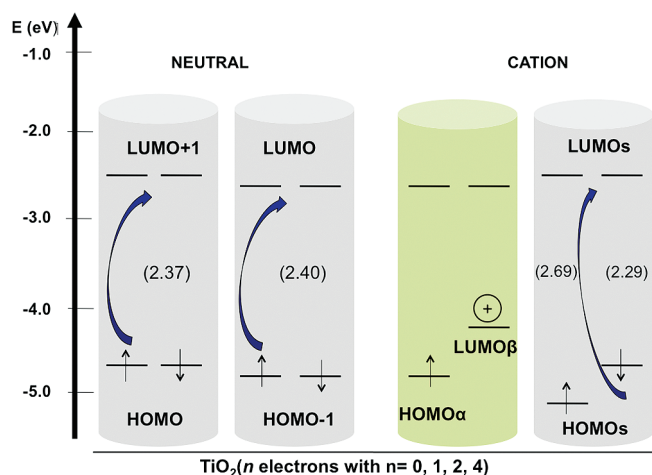


Figure 2. Schematic representation of the electronic structure of the neutral and cationic model systems employed, with the corresponding HOMO–LUMO gaps calculated at the B3LYP/6-31G* level in acetonitrile solution reported within parentheses. The following cases are examined: N/TiO₂(*n*) with *n* = 0, 1, 2, 4 and C/TiO₂(*n*) with *n* = 0, 1; see text for definitions. Values in parentheses are HOMO–LUMO gaps in eV.

$\Delta\mu_z$ should be almost equal to the total $|\Delta\mu|$, while in the latter, it is expected to be considerably smaller. As a matter of fact, we calculated $\Delta\mu_z$ of 15.0 D over a total $|\Delta\mu|$ of 45.7 D. In line with previous TD-DFT calculations,⁵⁴ the calculated $\Delta\mu_z$ is possibly overestimated compared to the experimental values. Although larger than the experimental estimate and the value reported in ref 24, the computed $\Delta\mu$ values confirm that being able to experimentally assess $\Delta\mu_z$ should allow us to gain insight into the relative orientation of the dye with respect to the semiconductor surface.

In the optimized dimeric structure, the molecules have an inclination with respect to the TiO₂ surface of about 43° (Figure 1a) and do lie not perfectly aligned, as was the case for the smaller D102 dye,⁵² but they turn out to be separated by one row of Ti atoms, with a distance between the carboxylic carbons of the two dyes amounting to 11.1 Å. As reported elsewhere for similar dyes,⁵⁵ the interaction between the deprotonated molecules and the TiO₂ surface is rather strong, with average calculated distances between the carboxylic oxygens and the TiO₂ surface (O–Ti bond) of 2.05–2.1 Å. A binding energy of 1.07 eV is computed for the similar D102 dye on TiO₂,⁵² in line with the rather strong dye/semiconductor interaction that might be inferred from the bond distances. It is worthwhile to point out that the importance of assessing the binding mode of D149 also opens the possibility to gain insight into the adsorption mode of related sensitizers bearing the same rhodanine-3-acetic acid group as the acceptor/anchoring moiety, such as, for instance, the rhodanine L0-L3 series by Marinado et al.⁵⁰ for which a similar bidentate binding can be expected.

Figure 2 shows a schematic representation of the model employed to simulate the Stark shifts along with the representative calculated electronic structures. The different cases examined here are (i) left side, the neutral dye dimer, hereafter labeled N/TiO₂(0), with its two quasi-degenerate intramolecular CT (ICT) transitions, 388(HOMO) → 390(LUMO+1) and 387-(HOMO–1) → 389(LUMO) and (ii) right side, the cationic system originating from removal of one electron from the dye

dimer, with the charge hole localized on the left monomer (orbital 388β) and the HOMO → LUMO excitation occurring in the neutral dye on the right side in the presence of the charge hole. Using this cationic dimer, indicated as C/TiO₂(0), one can thus precisely evaluate how the presence of the positive charge, localized on one dye molecule, perturbs the absorption spectrum of the neutral adjacent dye. As a further expansion of our model, we also simulate the case of an electron injected from the dye to the semiconductor manifold of unoccupied states, C/TiO₂(1), so that the cooperative effect of the neighboring dye cation and of the charge in the underlying TiO₂ semiconductor can be accounted for. The effect of injected charge into the TiO₂ semiconductor is simulated here by simply smearing the negative charge corresponding to *n* electrons over all Ti atoms in an evenly distributed fashion. Recalling that the nature of the unoccupied TiO₂ states is mainly Ti-*t*_{2g} delocalized states, this simplification seems fully justified. This is a simplified method to account for the injected charge into the semiconductor, which can however be effectively coupled to excited-state TD-DFT calculations. Finally, as hypothesized by Cappel et al.²⁷ and Anderson et al.,²⁸ local accumulation or depletion of electronic charge into the TiO₂ nanoparticles could also affect in some measure the spectroscopic properties of the absorbed sensitizers, yielding the measured spectral shifts. We, hence, examine here the effect on the absorption spectrum of the neutral dimeric system arising from an incremental “local” charge accumulation in the oxide CB, considering the cases of N/TiO₂(*n*), with *n* = 1, 2, and 4.

The UV absorption spectra for the dimeric (2,2)-D149 system have been simulated using the B3LYP exchange-correlation functional.⁵⁶ As previously shown,^{52,57,58} while underestimating the CT states of most of the push–pull organic chromophores,⁵⁹ conventional hybrid functionals successfully reproduce the optical properties of indoline dyes. For the deprotonated N/TiO₂–(0) dimer in acetonitrile, we calculated two intense quasi-degenerate transitions at 2.07 and 2.09 eV, with oscillator strengths of 0.76 and 0.83, respectively, which essentially correspond to the ICT excitation of the two monomers (see representative molecular orbitals in Figure 3). As already observed for the isolated dye monomer for which we calculated an absorption maximum of 2.06 eV,⁵² the excitation energy values for the dimers turn out to be somewhat lower than the experimental absorption maximum located at 2.36 eV.⁷ This calculated underestimate of the TD-DFT excitation energies compared to the experimental absorption maxima was traced back to the level of calculation adopted for the geometry optimization⁵² and was corrected by reoptimizing the monomer geometry by B3LYP, obtaining an absorption maximum of 2.23 eV.⁵² As we are interested here in relative band shifts rather than in absolutely reproducing excitation energies, we shifted by 0.28 eV the calculated spectra in order to exactly reproduce the experimental position of the absorption maximum for the neutral system on TiO₂.²⁴

If the electronic coupling between the two molecules is weak, as was shown to be the case for (2,2)-D149,⁵² upon extraction of one electron, we can expect the hole to be localized on a single dye molecule, yielding the cationic dimer schematically represented on the right side of Figure 2 and whose frontier molecular orbitals, split in their α and β components, are displayed on the right side of Figure 3. The electron is indeed extracted from the 388β spin–orbital, corresponding to the HOMO of the left monomer. The ICT transition on the right neutral monomer is

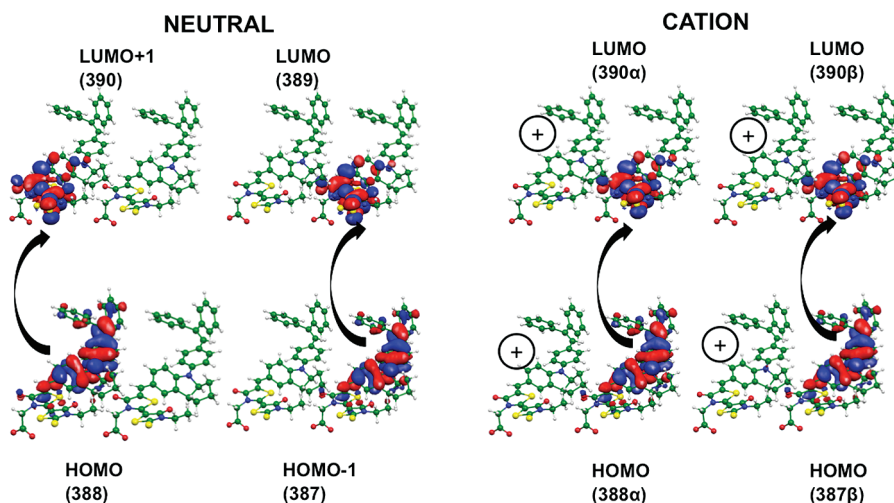


Figure 3. Isodensity surface plots of the frontier molecular orbitals for the (2,2)-D149 neutral and cationic dimers calculated at the B3LYP/6-31G* level in acetonitrile. The two quasidegenerate HOMO \rightarrow LUMO+1 and HOMO-1 \rightarrow LUMO excitations are represented on the left side, whereas the HOMO \rightarrow LUMO transition localized on the neutral monomer in the presence of adjacent cation is depicted on the right side.

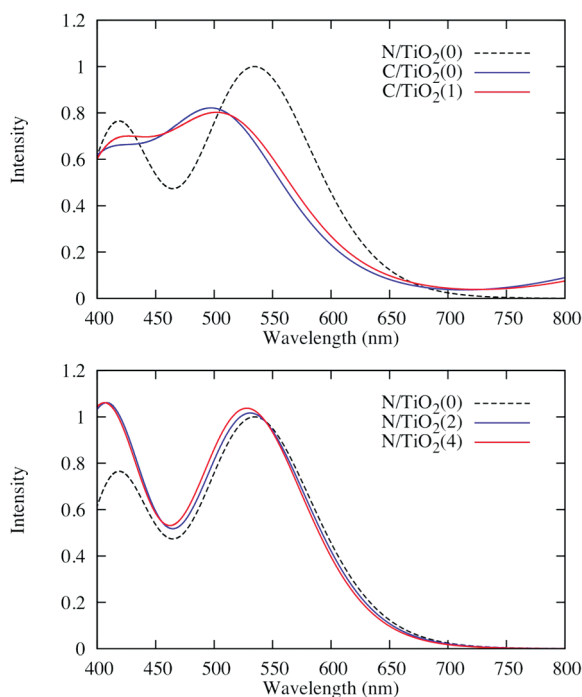


Figure 4. Absorption spectra in acetonitrile solution of (2,2)-D149 for the N/TiO₂(0), C/TiO₂(0), and C/TiO₂(1) cases (top) and N/TiO₂(0), N/TiO₂(2), and N/TiO₂(4) cases (bottom). The spectra, simulated by a Gaussian broadening with $\sigma = 0.20$ eV and normalized to the N/TiO₂(0) maximum intensity, have been shifted by 0.28 eV to make the experimental maximum of D149 and the calculated excitation coincident.

composed of the $388\alpha \rightarrow 390\alpha$ and $387\beta \rightarrow 390\beta$ excitations. For the corresponding HOMO/LUMO orbitals, the calculated energy gaps are 2.69 and 2.29 eV, respectively, to be compared to the gap of 2.39 eV computed for the neutral system. The hole generation from the occupied 388β spin-orbital clearly yields a sizable stabilization of the α counterpart, shifting down the 388α orbital from -4.78 (average value in the neutral dimer) to -5.28 eV while producing a smaller effect on the LUMO,

Table 1. Calculated Absorption Maxima (nm) in Acetonitrile and Corresponding Energy Shifts (eV) for the N/TiO₂(0), C/TiO₂(0), C/TiO₂(1), N/TiO₂(1), N/TiO₂(2), and N/TiO₂(4) Cases^a

| system | λ_{\max} (nm) | Stark shift (eV) |
|------------------------|-----------------------|------------------|
| N/TiO ₂ (0) | 526 | |
| C/TiO ₂ (0) | 489 | 0.18 |
| C/TiO ₂ (1) | 494 | 0.15 |
| N/TiO ₂ (1) | 523 | 0.01 |
| N/TiO ₂ (2) | 522 | 0.02 |
| N/TiO ₂ (4) | 519 | 0.03 |

^a The calculated spectra are shifted by 0.28 eV to make the calculated and experimental maxima coincident.

which shifts from -2.41 in the neutral to -2.58 eV in the cationic system.

In line with experimental evidence,²⁴ the calculated absorption spectra plotted in Figure 4 clearly show that for all of the examined model cases, a blue shift in the absorption, even if of different magnitude, is predicted. In Table 1, we report the computed band shifts corresponding to the various cases examined relative to the neutral dimer. Interestingly, what is apparent from our results is that taken alone, the effect of the charge into the TiO₂ is rather modest; the Stark shifts calculated for the N/TiO₂(n) systems increase linearly with increasing charge in TiO₂, that is, n going from 1 to 4. The absorption spectra displayed on the bottom of Figure 4 also reveal a linear slight rise in the absorption intensity as n increases, similarly to what was found in ref 24. According to our model, therefore, the injected charge seems to be only in part responsible for the sizable observed spectral changes. In fact, when the presence of the adjacent oxidized molecule is taken into account, the computed absorption blue shift is remarkable, and such optical response is consistent with the appreciable Stark shifts experimentally measured.²⁴ The absorption maximum moves from 526 to 494 nm, with a shift of 0.15 eV, in the case of the C/TiO₂(1) system and to 489 nm, with a shift of 0.18 eV, for C/TiO₂(0). In line with the TD-DFT calculations performed by Cappel et al.,²⁴

we also computed a blue shift of 0.1 eV when an external electric field with a strength of $5 \times 10^8 \text{ V m}^{-1}$ was applied in the z direction (normal to the TiO_2 surface).

Here, a remark concerning the intensity of the calculated spectra shown in the top plot of Figure 4 is necessary; as a consequence of the Stark effect, the experimental absorption spectra appear blue-shifted and with an increased intensity, while the bands calculated for the $\text{C/TiO}_2(n)$ systems are both less intense than that of $\text{N/TiO}_2(0)$. Actually, one should keep in mind that a comparison among the computed oscillator strengths for $\text{N/TiO}_2(0)$ and $\text{C/TiO}_2(n)$ is not meaningful because the neutral and the cationic systems have a different number of electrons.

The results presented here, therefore, nicely account for the experimentally observed band shifts and, more importantly, indicate that the effect of positive charge localized on adjacent dyes seems to play a major role in blue-shifting the absorption spectrum of neutral dyes, as a consequence of the strong intermolecular electrostatic interaction. In this respect, we speculate that the aggregation pattern of the investigated organic dyes and their tendency to form packed layers might influence to some extent the magnitude of the Stark shift.

In summary, we have presented a computational investigation, based on DFT/TD-DFT calculations, aimed to model the Stark shifts induced by local electric fields, arising upon dye oxidation/electron injection, observed in DSCs based on the indoline D149 sensitizer. Considering the most stable dimeric configuration of D149⁵² adsorbed on a (101) anatase $(\text{TiO}_2)_{82}$ cluster, we have examined the effect of various contributions, (i) an oxidized adjacent sensitizer, (ii) an incremental accumulation of charge into the TiO_2 semiconductor, and (iii) the simultaneous presence of the adjacent cation and an electron injected into the semiconductor. The results presented here clearly show that the positive charge localized on the adjacent sensitizer is a major cause for the observed spectral changes, yielding a Stark shift of 0.15–0.18 eV, fully consistent with the experimental measurements. The role of the injected charge was shown to be less relevant because also in the case of a charge of four electrons spread into the oxide nanocluster, the calculated blue shift was only 0.03 eV. Obviously, we cannot exclude that trap states in the semiconductor, which might induce electron localization nearby the absorbing dye, might play a role in enhancing the effect of injected charge.

We also have discussed the anchoring mode of D149 to TiO_2 , confirming a bidentate binding and calculating an inclination of about 43° of the molecule with respect to the surface; this is in line with the conclusion based on the determination of the change of the dipole moment between the ground and excited states reported in ref 24.

In conclusion, the present results show that our high-level computational methodologies together with the use of realistic models can quantitatively reproduce and elucidate the mechanism of a complex and not yet completely understood phenomenon such as the origin and the effect of local electric fields on the functioning of DSC devices.

MODELS AND COMPUTATIONAL DETAILS

The simplest model to simulate the Stark shifts, possibly induced by the electron injection from the excited state of the dye into the semiconductor CB and by the presence of oxidized neighboring dyes, consists of two D149 molecules adsorbed on a

TiO_2 surface. This rather complex system is sufficiently realistic but tractable by high-level ab initio calculations. Exploiting the results of our previous work on the aggregation of D149 on TiO_2 ,⁵² here, we take the optimized molecular structure of the most stable dimeric arrangement on D149 adsorbed onto a (101) $(\text{TiO}_2)_{82}$ anatase slab of $\sim 4 \text{ nm}^2$ area (Figure 1), termed (2,2)-D149.⁵² As we have previously shown, the rather bulky 2-rhodanine rings in the acceptor moiety of D149 do not allow a perfect stacking between the π -systems, as was instead the case of the smaller D102 dye; therefore, the molecules lie separated by one row of Ti atoms (see Figure 1). The geometry of this system was optimized by the Car–Parrinello (CP) method⁶⁰ using the PBE exchange-correlation functional,⁶¹ a plane-wave basis set, and ultrasoft pseudopotentials.^{62,63}

Following the procedure set up in ref 52, the absorption spectra simulations have been carried out in acetonitrile solution on the optimized structure of the adsorbed deprotonated dimer obtained by removing the $(\text{TiO}_2)_{82}$ cluster. For the TD-DFT calculations, performed with the Gaussian03 code,⁶⁴ the hybrid B3LYP exchange-correlation functional⁵⁶ and the standard 6-31G* basis set have been employed and the solvation effects included by means of the conductor-like polarizable continuum model (C-PCM).^{65,66} To mimic the electrons injected into the oxide CB, that is, into the titanium 3d orbitals, we put point charges,^{67,68} for a total charge of -1 , -2 , and -4 , on the Ti atoms positions in the original $(\text{TiO}_2)_{82}$ cluster; therefore, in each position, we have a point charge of $-1/82$, $-2/82$, and $-4/82$ for $\text{TiO}_2(1)$, $\text{TiO}_2(2)$, and $\text{TiO}_2(4)$, respectively. For the $\text{C/TiO}_2(n)$ cases, we computed the 70 lowest singlet excited states, while for the $\text{N/TiO}_2(n)$ ones, the calculations were limited to the 10 lowest singlet excitations; the UV absorption spectra were then simulated using a Gaussian broadening with $\sigma = 0.20 \text{ eV}$.

AUTHOR INFORMATION

Corresponding Author

*E-mail: filippo@thch.unipg.it.

ACKNOWLEDGMENT

We thank FP7-NMP-2009 Project 246124 “SANS” and Istituto Italiano di Tecnologia, Project Seed 2009 “HELYOS” for financial support.

REFERENCES

- (1) Hagfeldt, A.; Boschloo, G.; Sun, L.; Kloo, L.; Pettersson, H. Dye-Sensitized Solar Cells. *Chem. Rev.* **2010**, *110*, 6595–6663.
- (2) O'Regan, B.; Grätzel, M. A Low-Cost, High-Efficiency Solar Cell Based on Dye-Sensitized Colloidal TiO_2 Films. *Nature* **1991**, *353*, 737–740.
- (3) Nazeeruddin, M. K.; De Angelis, F.; Fantacci, S.; Selloni, A.; Viscardi, G.; Liska, P.; Ito, S.; Takeru, B.; Grätzel, M. Combined Experimental and DFT-TDDFT Computational Study of Photoelectrochemical Cell Ruthenium Sensitizers. *J. Am. Chem. Soc.* **2005**, *127*, 16835–16847.
- (4) Grätzel, M. Recent Advances in Sensitized Mesoscopic Solar Cells. *Acc. Chem. Res.* **2009**, *42*, 1788–1798.
- (5) Grätzel, M. Conversion of Sunlight to Electric Power by Nanocrystalline Dye-Sensitized Solar Cells. *J. Photochem. Photobiol. A* **2004**, *164*, 3–14.
- (6) Hara, K.; Kurashige, M.; Ito, S.; Shinpo, A.; Suga, S.; Sayama, K.; Arakawa, H. Novel Polyene Dyes for Highly Efficient Dye-Sensitized Solar Cells. *Chem. Commun.* **2003**, 252–253.

- (7) Horiuchi, T.; Miura, H.; Sumioka, K.; Uchida, S. High Efficiency of Dye-Sensitized Solar Cells Based on Metal-Free Indoline Dyes. *J. Am. Chem. Soc.* **2004**, *126*, 12218–12219.
- (8) Kim, S.; Lee, J. K.; Kang, S. O.; Ko, J.; Yum, J. H.; Fantacci, S.; De Angelis, F.; Di Censo, D.; Nazeeruddin, M. K.; Grätzel, M. Molecular Engineering of Organic Sensitizers for Solar Cell Applications. *J. Am. Chem. Soc.* **2006**, *128*, 16701–16707.
- (9) Hagberg, D. P.; Edvinsson, T.; Marinado, T.; Boschloo, G.; Hagfeldt, A.; Sun, L. C. A Novel Organic Chromophore for Dye-Sensitized Nanostructured Solar Cells. *Chem. Commun.* **2006**, 2245–2247.
- (10) Ito, S.; Zakeeruddin, S. M.; Humphry-Baker, R.; Liska, P.; Charvet, R.; Comte, P.; Nazeeruddin, M. K.; Péchy, P.; Takata, M.; Miura, H.; Uchida, S.; Grätzel, M. High-Efficiency Organic-Dye-Sensitized Solar Cells Controlled by Nanocrystalline-TiO₂ Electrode Thickness. *Adv. Mater.* **2006**, *18*, 1202–1205.
- (11) Ito, S.; Miura, H.; Uchida, S.; Takata, M.; Sumioka, K.; Liska, P.; Comte, P.; Péchy, P.; Grätzel, M. High-Conversion-Efficiency Organic Dye-Sensitized Solar Cells with a Novel Indoline Dye. *Chem. Commun.* **2008**, 5194–5196.
- (12) Zhang, G.; Bala, H.; Cheng, Y.; Shi, D.; Lv, X.; Yu, Q.; Wang, P. High Efficiency and Stable Dye-Sensitized Solar Cells with an Organic Chromophore Featuring a Binary p-Conjugated Spacer. *Chem. Commun.* **2009**, 2198–2200.
- (13) Daeneke, T.; Kwon, T.-H.; Holmes, A. B.; Duffy, N. W.; Bach, U.; Spiccia, L. High-Efficiency Dye-Sensitized Solar Cells with Ferrocene-based electrolytes. *Nat. Chem.* **2011**, *3*, 213–217.
- (14) Feldt, S. M.; Cappel, U. B.; Johansson, E. M. J.; Boschloo, G.; Hagfeldt, A. Characterization of Surface Passivation by Poly(methylsiloxane) for Dye-Sensitized Solar Cells Employing the Ferrocene Redox Couple. *J. Phys. Chem. C* **2010**, *114*, 10551–10558.
- (15) Feldt, S. M.; Gibson, E. A.; Gabrielson, E.; Sun, L.; Boschloo, G.; Hagfeldt, A. Design of Organic Dyes and Cobalt Polypyridine Redox Mediators for High-Efficiency Dye-Sensitized Solar Cells. *J. Am. Chem. Soc.* **2010**, *132*, 16714–16724.
- (16) Cameron, P. J.; Peter, L. M.; Zakeeruddin, S. M.; Grätzel, M. Electrochemical Studies of the Co(III)/Co(II)(dbbp)₂ Redox Couple as a Mediator for Dye-Sensitized Nanocrystalline Solar Cells. *Coord. Chem. Rev.* **2004**, *248*, 1447–1453.
- (17) O'Regan, B.; Moser, J.; Anderson, M.; Grätzel, M. Vectorial Electron Injection into Transparent Semiconductor Membranes and Electric Field Effects on the Dynamics of Light-Induced Charge Separation. *J. Phys. Chem.* **1990**, *94*, 8720–8726.
- (18) Tachibana, Y.; Haque, S. A.; Mercer, I. P.; Moser, J. E.; Klug, D. R.; Durrant, J. R. Modulation of the Rate of Electron Injection in Dye-Sensitized Nanocrystalline TiO₂ Films by Externally Applied Bias. *J. Phys. Chem. B* **2001**, *105*, 7424–7431.
- (19) Eichberger, R.; Willig, F. Ultrafast Electron Injection from Excited Dye Molecules into Semiconductor Electrodes. *Chem. Phys.* **1990**, *141*, 159–173.
- (20) Boschloo, G.; Hagfeldt, A. Photoinduced Absorption Spectroscopy of Dye-Sensitized Nanostructured TiO₂. *Chem. Phys. Lett.* **2003**, *370*, 381–386.
- (21) Boschloo, G.; Hagfeldt, A. Photoinduced Absorption Spectroscopy as a Tool in the Study of Dye-Sensitized Solar Cells. *Inorg. Chim. Acta* **2008**, *361*, 729–734.
- (22) Ardo, S.; Sun, Y.; Castellano, F. N.; Meyer, G. J. Excited-State Electron Transfer from Ruthenium–Polypyridyl Compounds to Anatase TiO₂ Nanocrystallites: Evidence for a Stark Effect. *J. Phys. Chem. B* **2010**, *114*, 14596–14604.
- (23) Ardo, S.; Sun, Y.; Staniszewski, A.; Castellano, F. N.; Meyer, G. J. Stark Effects after Excited-State Interfacial Electron Transfer at Sensitized TiO₂ Nanocrystallites. *J. Am. Chem. Soc.* **2010**, *132*, 6696–6709.
- (24) Cappel, U. B.; Feldt, S. M.; Schoneboom, J.; Hagfeldt, A.; Boschloo, G. The Influence of Local Electric Fields on Photoinduced Absorption in Dye-Sensitized Solar Cells. *J. Am. Chem. Soc.* **2010**, *132*, 9096–9101.
- (25) Staniszewski, A.; Ardo, S.; Sun, Y.; Castellano, F. N.; Meyer, G. J. Slow Cation Transfer Follows Sensitizer Regeneration at Anatase TiO₂ Interfaces. *J. Am. Chem. Soc.* **2008**, *130*, 11586–11587.
- (26) Snaith, H. J.; Karthikeyan, C. S.; Petrozza, A.; Teuscher, J.; Moser, J. E.; Nazeeruddin, M. K.; Thelakkat, M.; Grätzel, M. High Extinction Coefficient “Antenna” Dye in Solid-State Dye-Sensitized Solar Cells: A Photophysical and Electronic Study. *J. Phys. Chem. C* **2008**, *112*, 7562–7566.
- (27) Cappel, U. B.; Gibson, E. A.; Hagfeldt, A.; Boschloo, G. Dye Regeneration by Spiro-MeOTAD in Solid State Dye-Sensitized Solar Cells Studied by Photoinduced Absorption Spectroscopy and Spectroelectrochemistry. *J. Phys. Chem. C* **2009**, *113*, 6275–6281.
- (28) Anderson, A. Y.; Barnes, P. R. F.; Durrant, J. R.; O'Regan, B. Simultaneous Transient Absorption and Transient Electrical Measurements on Operating Dye-Sensitized Solar Cells: Elucidating the Intermediates in Iodide Oxidation. *J. Phys. Chem. C* **2010**, *114*, 1953–1958.
- (29) Stark, J. Observation of the Separation of Spectral Lines by an Electric Field. *Nature* **1914**, *401*, 401.
- (30) Boxer, S. G. Stark Realities. *J. Phys. Chem. B* **2009**, *113*, 2972–2983.
- (31) Bublitz, G. U.; Boxer, S. G. Stark Spectroscopy: Applications in Chemistry, Biology, and Materials Science. *Ann. Rev. Phys. Chem.* **1997**, *48*, 213–242.
- (32) Norris, D. J.; Sacra, A.; Murray, C. B.; Bawendi, M. G. Measurement of the Size Dependent Hole Spectrum in CdSe Quantum Dots. *Phys. Rev. Lett.* **1994**, *72*, 2612–2615.
- (33) Szczepankiewicz, S. H.; Moss, J. A.; Hoffmann, M. R. Electron Traps and the Stark Effect on Hydroxylated Titania Photocatalysts. *J. Phys. Chem. B* **2002**, *106*, 7654–7658.
- (34) Oh, D. H.; Boxer, S. G. Stark Effect Spectra of Ru(diimine)₃²⁺ Complexes. *J. Am. Chem. Soc.* **1989**, *111*, 1130–1131.
- (35) Vance, F. W.; Hupp, J. T. Probing the Symmetry of the Nonlinear Optic Chromophore Ru(*trans*-4,4'-diethylaminostyryl-2,2'-bipyridine)₃²⁺: Insight from Polarized Hyper-Rayleigh Scattering and Electroabsorption (Stark) Spectroscopy. *J. Am. Chem. Soc.* **1999**, *121*, 4047–4053.
- (36) Riesen, H.; Wallace, L.; Krausz, E. Dynamical Processes in the Lowest-Excited Triplet Metal-to-Ligand Charge Transfer States of Ruthenium and Osmium Diimine Complexes in Crystals. *Int. Rev. Phys. Chem.* **1997**, *16*, 291–359.
- (37) Qin, P.; Zhu, H.; Edvinsson, T.; Boschloo, G.; Hagfeldt, A.; Su, L. Design of an Organic Chromophore for p-Type Dye-Sensitized Solar Cells. *J. Am. Chem. Soc.* **2008**, *130*, 8570–8571.
- (38) Hagfeldt, A.; Grätzel, M. Light-Induced Redox Reactions in Nanocrystalline Systems. *Chem. Rev.* **1995**, *95*, 49–68.
- (39) Falaras, P. Synergetic Effect of Carboxylic Acid Functional Groups and Fractal Surface Characteristics for Efficient Dye Sensitization of Titanium Oxide. *Sol. Energy Mater. Sol. Cells* **1998**, *53*, 163–175.
- (40) Finnie, K. S.; Bartlett, J. R.; Woolfrey, J. L. Vibrational Spectroscopic Study of the Coordination of (2,2'-Bipyridyl-4,4'-dicarboxylic acid)ruthenium(II) Complexes to the Surface of Nanocrystalline Titania. *Langmuir* **1998**, *14*, 2744–2749.
- (41) Srinivas, K.; Yesudas, K.; Bhanuprakash, K.; Rao, V. J.; Giribabu, L. A Combined Experimental and Computational Investigation of Anthracene Based Sensitizers for DSSC: Comparison of Cyanoacrylic and Malonic Acid Electron Withdrawing Groups Binding onto the TiO₂ Anatase (101) Surface. *J. Phys. Chem. C* **2009**, *113*, 20117–20126.
- (42) Hara, K.; Sato, T.; Katoh, R.; Furube, A.; Yoshihara, T.; Murai, M.; Kurashige, M.; Ito, S.; Shinpo, A.; Suga, S. Novel Conjugated Organic Dyes for Efficient Dye-Sensitized Solar Cells. *Adv. Funct. Mater.* **2005**, *15*, 246–252.
- (43) Hara, K.; Sato, T.; Katoh, R.; Furube, A.; Ohga, Y.; Shinpo, A.; Suga, S.; Sayama, K.; Sugihara, H.; Arakawa, H. Molecular Design of Coumarin Dyes for Efficient Dye-Sensitized Solar Cells. *J. Phys. Chem. B* **2003**, *107*, 597–606.
- (44) Ganbold, E.-O.; Lee, Y.; Lee, K.; Kwon, O.; Joo, S.-W. Interfacial Behavior of Benzoic Acid and Phenylphosphonic Acid on Nanocrystalline TiO₂ Surfaces. *Chem. Asian J.* **2010**, *5*, 852–858.

- (45) Nazeeruddin, M. K.; Humphry-Baker, R.; Liska, P.; Grätzel, M. Investigation of Sensitizer Adsorption and the Influence of Protons on Current and Voltage of a Dye-Sensitized Nanocrystalline TiO₂ Solar Cell. *J. Phys. Chem. B* **2003**, *107*, 8981–8987.
- (46) Lee, K. E.; Gomez, M. A.; Elouatik, S.; Demopoulos, G. P. Further Understanding of the Adsorption Mechanism of N719 Sensitizer on Anatase TiO₂ Films for DSSC Applications Using Vibrational Spectroscopy and Confocal Raman Imaging. *Langmuir* **2010**, *26*, 9575–9583.
- (47) Pérez León, C.; Kador, L.; Peng, B.; Thelakkat, M. Characterization of the Adsorption of Ru-bpy Dyes on Mesoporous TiO₂ Films with UV–Vis, Raman, and FTIR Spectroscopies. *J. Phys. Chem. B* **2006**, *110*, 8723–8730.
- (48) Deacon, G. B.; Phillips, R. J. Relationships Between the Carbon–Oxygen Stretching Frequencies of Carboxylate Complexes and the Type of Carboxylate Coordination. *Coord. Chem. Rev.* **1980**, *33*, 227–250.
- (49) Johansson, E. M. J.; Edvinsson, T.; Odelius, M.; Hagberg, D. P.; Sun, L.; Hagfeldt, A.; Siegbahn, H.; Rensmo, H. Electronic and Molecular Surface Structure of a Polyene–Diphenylamine Dye Adsorbed from Solution onto Nanoporous TiO₂. *J. Phys. Chem. C* **2007**, *111*, 8580–8586.
- (50) Marinado, T.; Hagberg, D.; Hedlund, M.; Edvinsson, T.; Johansson, E.; Boschloo, G.; Rensmo, H.; Brinck, T.; Sun, L.; Hagfeldt, A. Rhodanine Dyes for Dye-Sensitized Solar Cells: Spectroscopy, Energy Levels and Photovoltaic Performance. *Phys. Chem. Chem. Phys.* **2009**, *11*, 133–141.
- (51) Hahlin, M.; Johansson, E.; Plogmaker, S.; Odelius, M.; Sun, L.; Siegbahn, H.; Rensmo, H. Electronic and Molecular Structures of Organic Dye/TiO₂ Interfaces for Solar Cell Applications: A Core Level Photoelectron Spectroscopy Study. *Phys. Chem. Chem. Phys.* **2010**, *12*, 1507–1517.
- (52) Pastore, M.; De Angelis, F. Aggregation of Organic Dyes on TiO₂ in Dye-Sensitized Solar Cells Models: An Ab Initio Investigation. *ACS Nano* **2010**, *4*, 556–562.
- (53) Howie, W. H.; Claeysens, F.; Miura, H.; Peter, L. M. Characterization of Solid-State Dye-Sensitized Solar Cells Utilizing High Absorption Coefficient Metal-Free Organic Dyes. *J. Am. Chem. Soc.* **2008**, *130*, 1367–1375.
- (54) De Angelis, F.; Fantacci, S.; Sgamellotti, A.; Cariati, F.; Roberto, D.; Tessore, F.; Ugo, R. A Time-Dependent Density Functional Theory Investigation on the Nature of the Electronic Transitions Involved in the Nonlinear Optical Response of [Ru(CF₃CO₂)₃T] (T = 4'-(C₆H₄-p-NBu₂)-2,2':6',2''-terpyridine). *Dalton Trans.* **2006**, 852–859.
- (55) Chen, P.; Yum, J. H.; Angelis, F. D.; Mosconi, E.; Fantacci, S.; Moon, S.-J.; Baker, R. H.; Ko, J.; Nazeeruddin, M. K.; Grätzel, M. High Open-Circuit Voltage Solid-State Dye-Sensitized Solar Cells with Organic Dye. *Nano Lett.* **2009**, *9*, 2487–2492.
- (56) Becke, A. D. A New Mixing of Hartree–Fock and Local Density-Functional Theories. *J. Chem. Phys.* **1993**, *98*, 1372–1377.
- (57) Jose, R.; Kumar, A.; Thavasi, V.; Fujihara, K.; Uchida, S.; Ramakrishna, S. Relationship Between the Molecular Orbital Structure of the Dyes and Photocurrent Density in the Dye-Sensitized Solar Cells. *Appl. Phys. Lett.* **2008**, *93*, 023125.
- (58) Le Bahers, T.; Pauporté, T.; Scalmani, G.; Adamo, C.; Ciofini, I. A TD-DFT Investigation of Ground and Excited State Properties in Indoline Dyes Used for Dye-Sensitized Solar Cells. *Phys. Chem. Chem. Phys.* **2009**, *11*, 11276–11284.
- (59) Pastore, M.; Mosconi, E.; De Angelis, F.; Grätzel, M. A Computational Investigation of Organic Dyes for Dye-Sensitized Solar Cells: Benchmark, Strategies, and Open Issues. *J. Phys. Chem. C* **2010**, *114*, 7205–7212.
- (60) Car, R.; Parrinello, M. Unified Approach for Molecular Dynamics and Density-Functional Theory. *Phys. Rev. Lett.* **1985**, *55*, 2471–2474.
- (61) Perdew, J. P.; Burke, K.; Ernzerhof, M. Generalized Gradient Approximation Made Simple. *Phys. Rev. Lett.* **1996**, *77*, 3865–3868.
- (62) Pasquarello, A.; Laasonen, K.; Car, R.; Lee, C.; Vanderbilt, D. Ab Initio Molecular Dynamics for d-Electron Systems: Liquid Copper at 1500 K. *Phys. Rev. Lett.* **1992**, *69*, 1982–1985.
- (63) Giannozzi, P.; Angelis, F. D.; Car, R. First-Principle Molecular Dynamics with Ultrasoft Pseudopotentials: Parallel Implementation and Application to Extended Bioinorganic Systems. *J. Chem. Phys.* **2004**, *120*, 5903–5915.
- (64) Frisch, M. J.; Trucks, G. W.; Schlegel, H. B.; Scuseria, G. E.; Robb, M. A.; Cheeseman, J. R.; Montgomery, J. A., Jr.; Vreven, T.; Kudin, K. N.; Burant, J. C.; Millam, J. M.; Gaussian 03, revision B.05; Gaussian, Inc.: Pittsburgh, PA, 2003.
- (65) Cossi, M.; Barone, V. Time-Dependent Density Functional Theory for Molecules in Liquid Solutions. *J. Chem. Phys.* **2001**, *115*, 4708–4717.
- (66) Cossi, M.; Rega, N.; Scalmani, G.; Barone, V. Structures, and Electronic Properties of Molecules in Solution with the C-PCM Solvation Model. *J. Comput. Chem.* **2003**, *24*, 669–681.
- (67) Hall, G. G.; Smith, C. M. Fitting Electron-Densities of Molecules. *Int. J. Quantum Chem.* **1984**, *88*, 4926–4933.
- (68) Smith, C. M.; Hall, G. G. Approximation of Electron-Densities. *Theor. Chem. Acc.* **1986**, *69*, 63–69.